Available online at www.sciencedirect.com

SciVerse ScienceDirect

Ceramics International 38 (2012) 3029–3037

CERAMICS INTERNATIONAL

www.elsevier.com/locate/ceramint

Study of structural, dielectric and electrical conduction behaviour of Gd substituted $CaCu_3Ti_4O_{12}$ ceramics

Raman Kashyap [a], O.P. Thakur [b], R.P. Tandon [a,*]

[a] Department of Physics and Astrophysics, University of Delhi, 110007, India

[b] Electroceramics Group, Solid State Physics Laboratory, Timarpur, Delhi 110054, India

Received 9 November 2011; received in revised form 30 November 2011; accepted 30 November 2011

Available online 8 December 2011

Abstract

Effect of Gd on microstructural, dielectric and electrical properties has been studied over wide temperature (300–500 K) and frequency range (100 Hz–1 MHz). Gd substitution in CCTO system results in decrease in the grain size and increase of Schottky potential barrier which causes lower value of dielectric constant. The dielectric constant remains nearly constant in temperature range 300–350 K. Doped samples show lower dielectric loss in middle frequency range (~10 kHz–1 MHz) at room temperature. The AC conductivity (σ_{ac}) obeys a power law, $\sigma_{ac} = Af^n$, where n is temperature dependent frequency exponent. The AC conductivity behaviour can be divided into three regions depending on conduction processes and the relevant charge transport mechanisms have been discussed.

Keywords: A. Powders: solid state reaction method; B. Grain boundaries; C. Dielectric properties; C. Electrical conductivity

1. Introduction

Recently calcium copper titanate (CCTO) has attracted attention due to colossal dielectric constant which remains almost constant over a wide temperature range (100–600 K) [1]. High dielectric constant leads to miniaturization of capacitive components in electronic devices. CCTO ($CaCu_3Ti_4O_{12}$) has body centred structure and has been placed in Im3 space group [2]. No change in crystal structure is observed down to 35 K [1]. Origin of giant dielectric constant in CCTO ($\sim 10^5$ for single crystal [1] and $\sim 10^4$ for polycrystalline [2]) has been enigmatic. Several mechanisms have been put forward to explain the origin of dielectric constant in CCTO [1–5]. Internal Barrier Layer Capacitance (IBLC) mechanism has been accepted as most plausible mechanism to explain origin of dielectric constant in these ceramics [3,4,6]. IBLC mechanism states that conducting grains and insulating grain boundaries give rise to high value of dielectric constant. Dielectric properties are observed to be processing conditions dependent [7]. Adams et al. [6] and Li et al. [8] proposed origin of semi-conductivity in CCTO in two ways. Adams et al. proposed that semi-conductivity originates from generation of oxygen vacancies, according to relation (Eq. (1))

$$O^{2-}(\text{lattice}) = (1/2)O(g) + 2e^- \quad (1)$$

where electrons enter the Ti 3d conduction band and this can be represented by Ti^{3+} in the formula $CaCu_3Ti^{4+}{}_{4-x}Ti^{3+}O_{12-x/2}$. Li et al. suggested that Cu^{2+} reduces to Cu^+ slightly and in order to maintain the oxidation state, a slight substitution of Ti^{4+} on Cu site compensates. Upon cooling Cu^+ oxidise to Cu^{2+}, releasing electrons into the Ti 3d conduction band as $Ca^{2+}(Cu^{2+}{}_{1-x}Ti^{4+}{}_x)_3(Ti^{4+}{}_{4-6x}Ti^{3+}{}_6)O_{12}$, where a very small amount of 'x' would affect conductivity without being detected in the X-ray diffraction data. CCTO shows the relaxor ferroelectric-like behaviour. Relaxor ferroelectrics are a class of compositionally dis-ordered, structurally frustrated incipient ferroelectrics [11]. CCTO ceramics are reported to exhibit the ferroelectric-like hysteresis loop [9,10], which is quite enigmatic as these ceramics have been assumed as non-ferroelectric owing to their bcc structure and Im3 space group [2].

Electrical measurements are most sensitive and versatile tool for the investigation of conduction mechanisms in solids. In the present paper, we study the role of Gd substitution on the structural, dielectric properties and electrical conduction

* Corresponding author. Tel.: +91 11 27667725x1367; fax: +91 11 27667061.
E-mail address: ram_tandon@hotmail.com (R.P. Tandon).

0272-8842/$36.00
doi:10.1016/j.ceramint.2011.11.085

behaviour of CCTO ceramics over wide temperature and frequency range.

2. Experimental details

Gd doped CCTO ceramics were prepared using solid state reaction method. Starting chemicals CuO (99%, Thomas Baker), TiO_2 (99%, Loba Chemie), $CaCO_3$ (99.5%, Sisco Research Laboratories Pte. Ltd.) and Gd_2O_3 (99.9%, Rare Earth Pte. Ltd.) were taken in stoichiometric amount according to $Ca_{1-3x/2}Gd_xCu_3Ti_4O_{12}$ ($x = 0$, 0.02, 0.04, 0.06, 0.08, 0.10). Samples with $x = 0.0$, 0.02, 0.04, 0.06, 0.08, and 0.10 will hereafter represented by S0, S2, S4, S6, S8 and S10 respectively. Powders were ball milled for 12 h in the distilled water with zirconia ball as grinding media. Milled powders were dried at 353 K for 24 h in oven. Dried powders were calcined at 1173 K for 5 h. Calcined powders were again ground using mortar-pestle. Room temperature X-ray diffraction (Bruker, D8 Discover) was done on calcined powders. Calcined powders were pressed into pellets of diameter 13 mm and thickness ~3–4 mm using polyvinyl alcohol (PVA) as binder. Green pellets were sintered at 1373 K using heating rate of 3 K/min for 2 h and then furnace cooled. These pellets were lapped to ~1 mm using silicon carbide abrasive powder and then cleaned using ultrasonicator for 15 min in distilled water. Pellets were dried at 363 K for 2 h. Microstructure and elemental analysis of fractured surfaces was recorded using Scanning Electron Microscope (SEM) (Zeiss, MA15) having EDS attachment. Gold was sputtered on both faces of the pellets for making electrical contacts. Impedance analyzer (Wayne Kerr 6500B) was used for the dielectric measurement as a function of frequency (100 Hz–1 MHz) and temperature (300–500 K).

3. Results and discussion

3.1. X-ray analysis

Fig. 1 shows the XRD patterns of Gd doped CCTO samples. XRD analysis confirms the single phase formation. Doped samples show minor 2θ shift in XRD peaks which may be attributed to difference in ionic radii of Ca (0.99 Å) and Gd (0.938 Å). Lattice parameters were found to be 7.389 Å, 7.461 Å, 7.443 Å, 7.451 Å, 7.441 Å, and 7.449 Å for samples S0, S2, S4, S6, S8 and S10 respectively.

3.2. Microstructure analysis

SEM images of fractured surface of pure and Gd doped ceramics are shown in Fig. 2a. Substitution of Gd in CCTO greatly affects the microstructure. Grain size decreases with increase in Gd content. Pure CCTO shows bigger grains (2–10 μm) whereas for subsequent doping concentrations, grain size reduces to range 0.5–2 μm. It is observed that for higher doping concentrations such as 8.10 mol%, grains start coalescing.

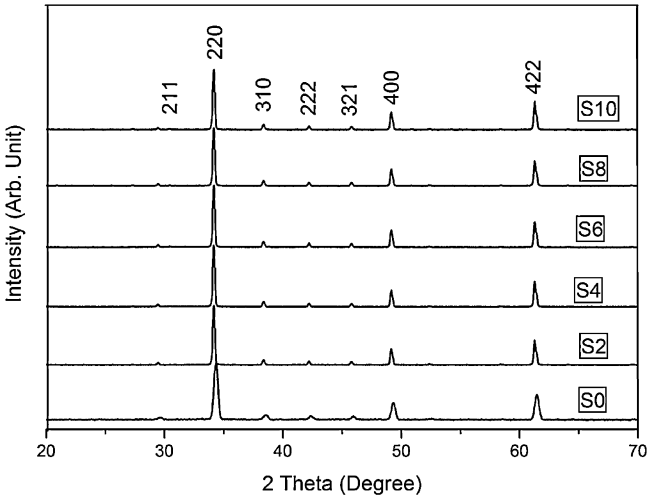

Fig. 1. XRD patterns of pure and Gd doped CCTO samples.

Energy spectrum (Fig. 2b) of elemental analysis of different regions of fractured surface of S0 and S10 doped samples gives insight into the proportion of different elements in different regions. Table 1 gives the wt% of elements found in different regions of Gd doped CCTO samples. It is observed that, with the increase of Gd content, grain and grain boundary also reflects increased concentration of Gd by EDS analysis. Major content of Gd was found in grain than in grain boundary region whereas no segregation of Cu was found in the grain boundary region. Intermediate Gd contents yielded same qualitative behaviour and hence not included in Fig. 2b.

3.3. Dielectric properties

Fig. 3a shows the frequency variation of real part of dielectric constant (ε') of Gd doped CCTO ceramics. Dielectric constant of doped samples S2, S4, S6, S8 and S10 at ~10 kHz reduces by an order when compared to pure CCTO at room temperature. Dielectric constant (ε') of pure sample shows decrease in value with increase in frequency whereas dielectric constant (ε') of Gd doped CCTO samples show feeble frequency dependence especially in the range 1 kHz–1 MHz. A sharp decrease of ε' is observed beyond 1 MHz. The drastic decrease in ε' at frequencies higher than 1 MHz, may indicate the presence of conductive grains [4]. At higher frequencies,

Table 1
Elemental proportion in samples S0 and S10 as per EDS analysis.

Sample name	Element	Grain (wt%)	Grain boundary (wt%)
S0	Ca	6.13	6.02
	Ti	30.66	31.28
	Cu	32.19	31.48
	O	31.03	31.22
S10	Ca	5.92	5.26
	Ti	31.18	32.00
	Cu	30.00	29.54
	O	31.03	31.22
	Gd	1.87	1.98

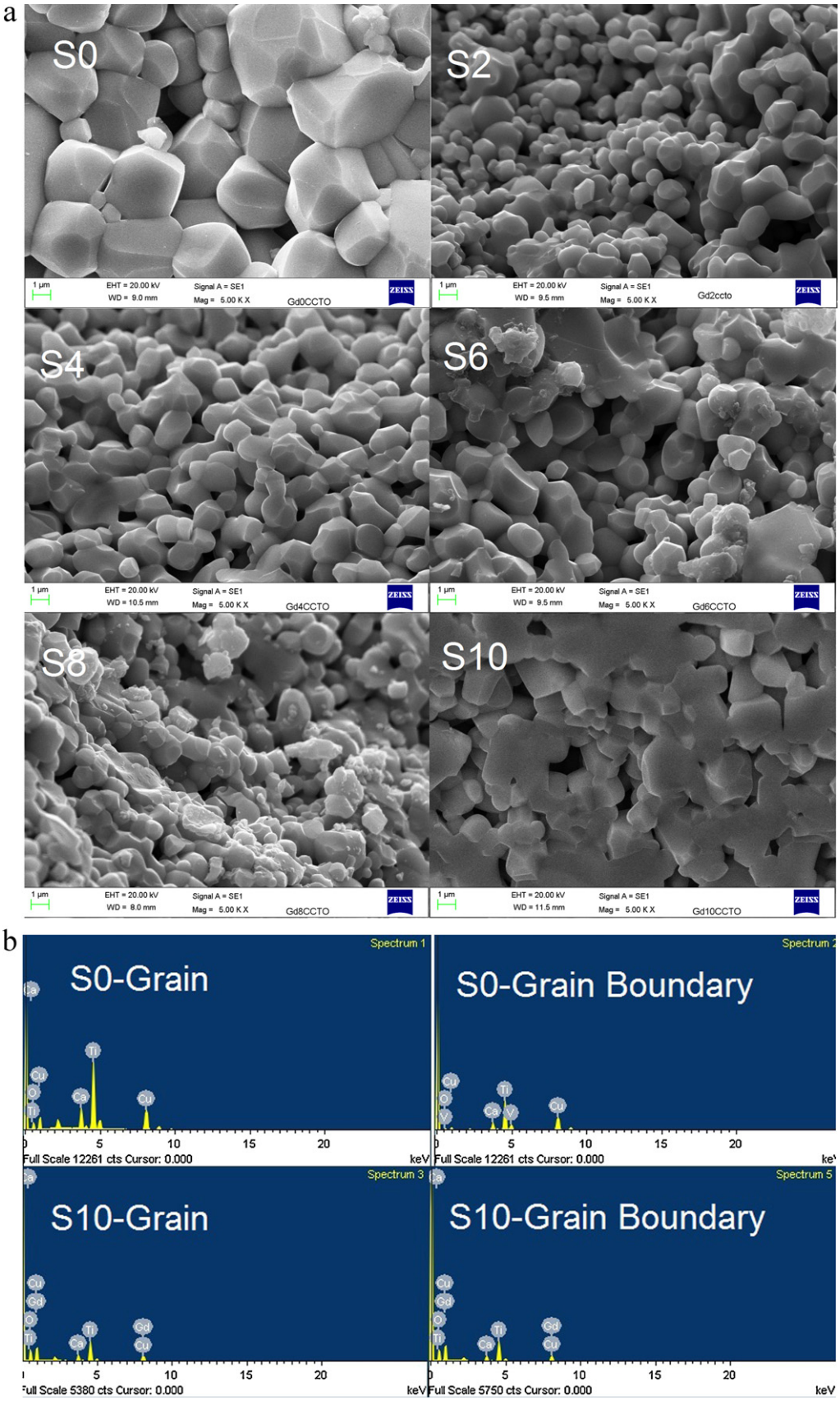

Fig. 2. (a) SEM images of pure and Gd doped samples. (b) EDS spectrum images of samples S0 and S10.

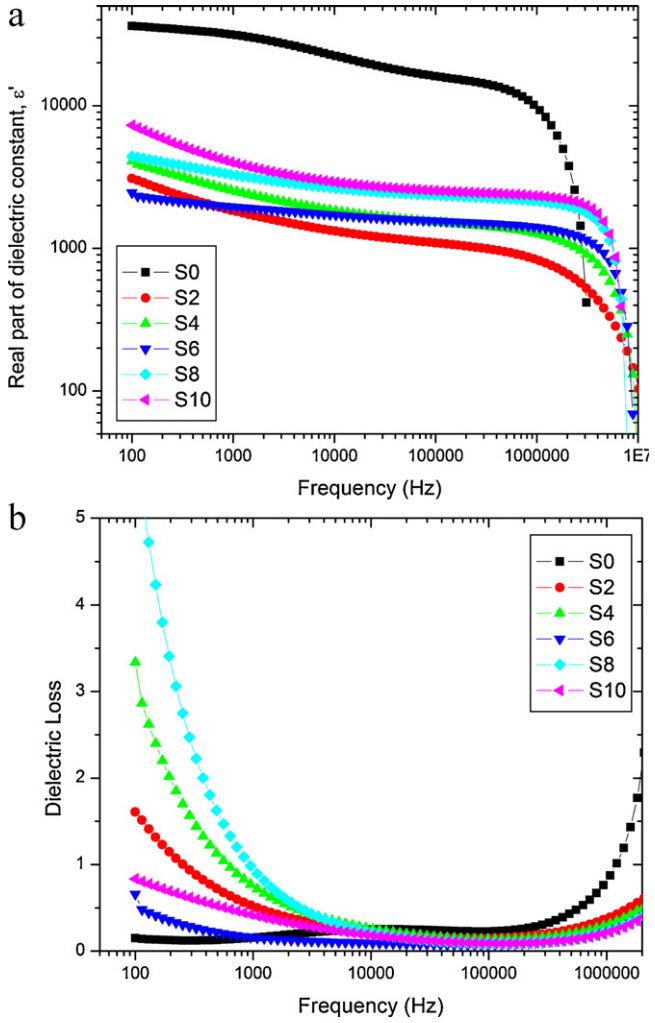

Fig. 3. (a) Variation of real part of dielectric constant ε' with frequency for pure and Gd doped samples. (b) Frequency dependence of dielectric loss for pure and Gd doped CCTO samples.

contribution is mainly from grain which results in low value of dielectric constant.

Debye-like relaxation is observed in the MHz region which may be inferred from sharp decrease in dielectric constant. High frequency dielectric relaxation may come from Maxwell–Wagner effect at grain boundary [12]. Maxwell–Wagner effect arises from the charge accumulation at interface of materials with different conductivities. It is reported that double (back-to-back) Schottky potential barriers are created at the interfaces between n-type grains due to charge trapping at acceptor states, resulting in bending of the conduction band across the grain boundaries [13]. Acceptor concentration N_s at the grain boundaries increases due to Gd doping, in terms of the following Eq. (2). Then Schottky potential ϕ_b may be enhanced resulting in a low dielectric constant by [14]:

$$\phi_b = \frac{eN_s^2}{8\varepsilon_o\varepsilon_r N_d} \tag{2}$$

where e is the electronic charge, N_s is the acceptor (surface charge) concentration, ε_o is vacuum permittivity, ε_r is the relative permittivity of the material, and N_d is the charge carrier concentration in grains.

Effect of grain size can be clearly seen on the values of dielectric constant. Gd substitution greatly reduces the value of dielectric constant (ε'). This may be attributed to decreasing size of grains with increasing Gd content. Pure CCTO shows larger grains and in turn high value of dielectric constant whereas Gd doped samples show smaller grains and lower value of dielectric constant.

It is believed that substitution of Gd in CCTO changes the charge distribution. In order to maintain the charge neutrality for each Gd substitution, one and half Ca is removed which results in generation of lattice vacancies. With increasing Gd content these vacancies also increase which may have detrimental effect on the dielectric constant.

Effect of Gd content on the frequency dependence of dielectric loss or tan(δ) is shown in Fig. 3b. Though, value of dielectric constant of CCTO decreased sharply as a result of doping, values of dielectric loss remains of same order for all the compositions.

Doped samples show lower dielectric loss in the middle frequency range (∼10 kHz–1 MHz). Variation in the values of

dielectric loss at lower frequencies may be attributed to electrode polarization. Fig. 4a shows the variation of real part of dielectric constant (ε') of pure and Gd doped ceramics with temperature at different frequencies.

Dielectric constant for CCTO ceramic shows weak temperature dependence with relaxor characteristics. With the substitution of Gd, relaxor behaviour becomes quite significant. Up to 2 mol% Gd, though magnitude of dielectric constant is decreased, relaxor behaviour is similar to that shown by pure CCTO. Further increase in Gd content, significantly enhances relaxor behaviour which may be attributed to compositional fluctuations as reported for other relaxor materials. Dependence of dielectric constant on temperature could be related to the excited deep trap states. At low temperature the interface is static because of the large relaxation time τ. With increasing T, this relaxation time

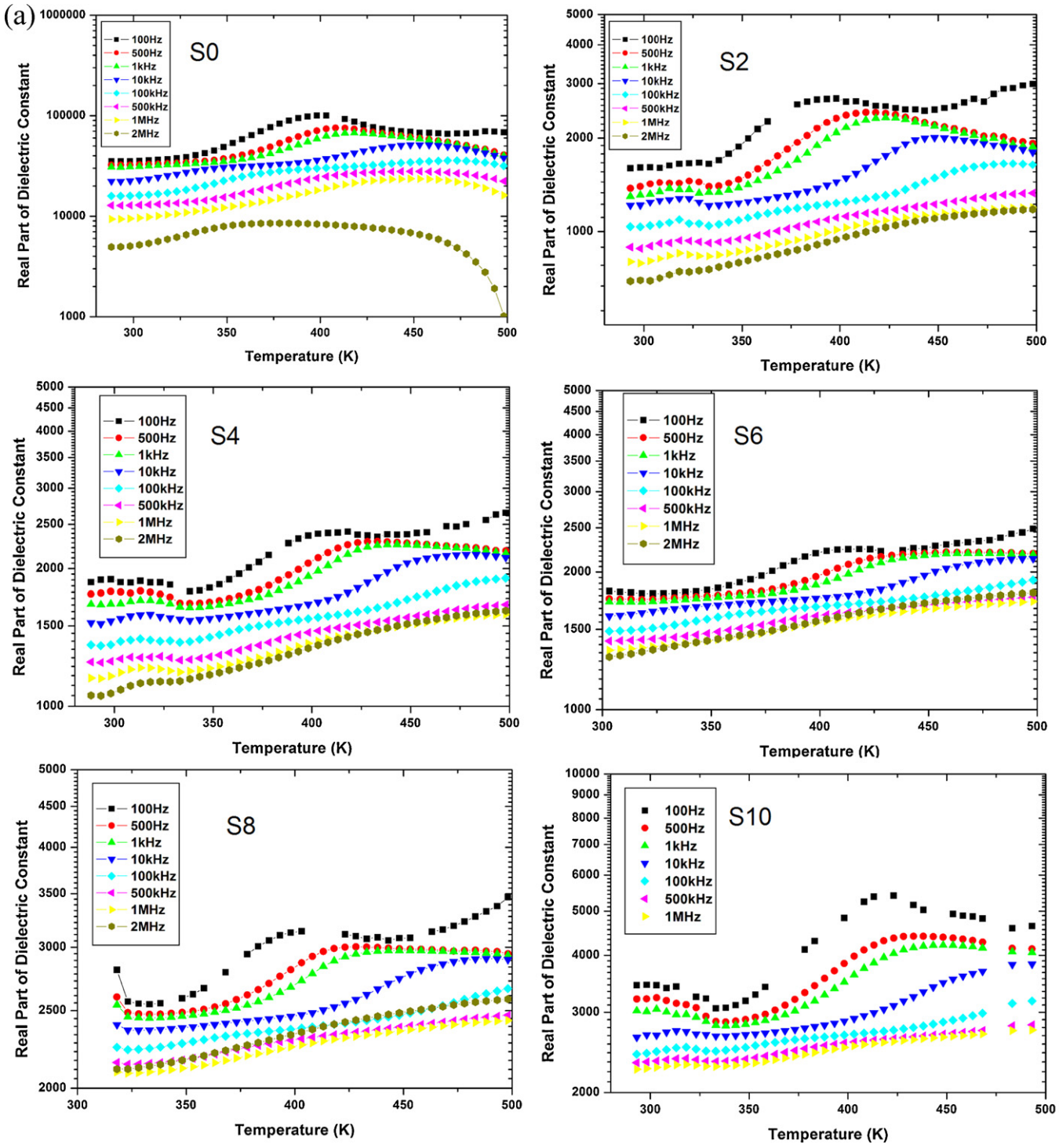

Fig. 4. (a) Variation of real part of dielectric constant ε' with temperature at different frequencies for pure and Gd doped samples.

decreases and for $\omega\tau < 1$ the capacitance maybe increased by the dynamic interface [13].

With increasing frequency, dielectric constant follows decreasing trend for all the samples. Relaxation peak shifts towards higher temperature side with increase in frequency. With increase in Gd content, relaxation peaks are observed to shift towards low temperature side. Samples show negligible variation in dielectric constant with temperature at 1 kHz and 10 kHz in the temperature range 300–350 K which may be utilized for device fabrication.

Two relaxation processes are observed from the frequency and temperature dependence of dielectric constant. Due to

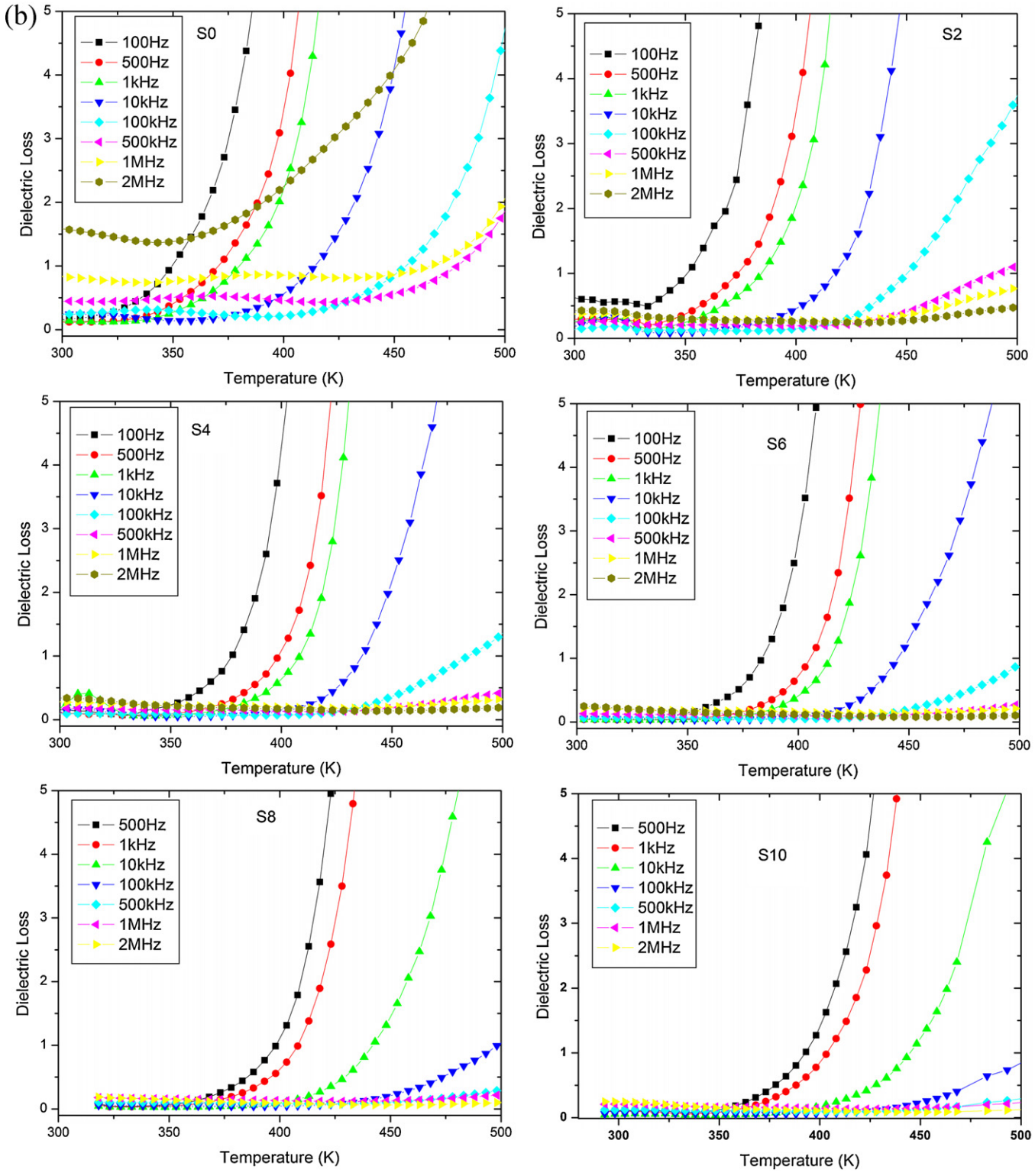

Fig. 4. (b) Variation of dielectric loss with temperature at different frequencies for pure and Gd doped CCTO samples.

frequency range available for measurement at room temperature, low frequency relaxation is not observed clearly but as temperature increases dielectric constant shows increase while the broad relaxation peak shifts towards higher temperature side with increase in frequency showing Debye-like relaxation. Low frequency relaxation is assumed to be associated with surface layers interfacial polarization [15]. Luo et al. [16] attributed low frequency relaxation to trap state related relaxation, which could be changed by electric conditioning but recover after releasing electric field. Therefore, the high dielectric constant, in the low frequency range, of CCTO could be attributed to the trap states which exist in the electrode surface. Since the time is long enough to let the traps response we get a huge permittivity at low frequency. Doped samples show relaxation at lower frequencies at high temperature which may be attributed to hopping of trapped carriers.

Effect of Gd content on the temperature dependence of dielectric loss or tan(δ) at different frequencies is shown in Fig. 4b. Doped samples show relatively smaller value of loss than pure CCTO in the temperature range 300–400 K at 1 kHz and 10 kHz. Dielectric loss increases rapidly with increase in temperature. This rapid shoot-off in dielectric loss shifts towards higher temperature side with increasing frequency.

3.4. AC conductivity

Total conductivity (σ) in solids can be expressed as

$$\sigma = \sigma_{ac} + \sigma_{dc} \tag{3}$$

where σ_{ac} is the AC conductivity which originates from hopping conduction and σ_{dc} is the DC conductivity which results from conduction band and. σ_{ac} is an increasing function of frequency in disordered solids [17]. In present work, σ_{ac} was calculated using relation

$$\sigma_{ac} = 2\pi f \varepsilon_o \varepsilon' \tan(\delta) \tag{4}$$

where f is frequency, ε_o is permittivity of vacuum, ε' is real part of dielectric constant and tan(δ) is the dielectric loss. Variation of σ_{ac} with frequency is shown in Fig. 5. AC power law shows the frequency dependence of σ_{ac} [18]

$$\sigma_{ac} = A f^n \tag{5}$$

where A is temperature dependent parameter, f is frequency and frequency exponent n is dimensionless correlation coefficient having values between 0 and 1. In Fig. 5 (inset shows S6), frequency range can be divided into three regions namely region I, II, and III. In region I, frequency is low, therefore, electric field does not influence the hopping conduction mechanism and conductance is almost equal to DC value. At low frequencies where the conductivity is constant, the transport takes place on infinite paths. In the region II, nonlinearity creeps in frequency variation of σ_{ac}. With further increase in frequency, conductivity increases linearly resulting in near constant loss (NCL) [19]. At high frequency, conduction may be due to electron hoping between adjacent Ti-Octahedron [17] and long range motion cannot occur. Increase in frequency increases hoping frequency and thereby increase in conductivity.

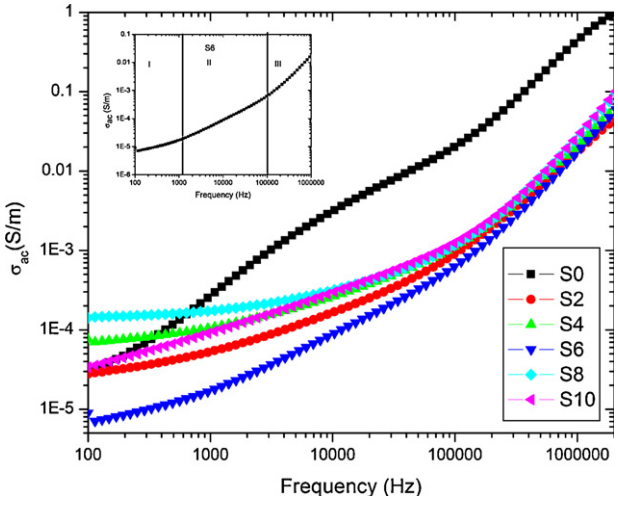

Fig. 5. Variation of AC conductivity σ_{ac} with frequency at different temperatures for pure and Gd doped CCTO samples.

The exponent n can be calculated as a function of temperature by plotting ln σ_{ac} vs ln f giving straight line with slope equal to exponent n. Values of exponent n for x = 0.0–0.1 are in the range 0.85–0.98. CCTO is an interesting material with semiconducting grains and insulating grain boundaries [3]. Substitution of Gd increases the resistivity of CCTO ceramics, as can be seen from Figs. 5 and 6. Variation of conductivity with frequency depends on number of potential barriers and their height. If a single charged species is assumed to move in an infinite lattice of identical potential wells, the σ_{ac} is expected to be independent of frequency. In case of single particle hopping to and fro in a double well with infinite height, conductivity will increase and saturates at high frequency [20].

Arrhenius plot for 6 mol% Gd in CCTO at different frequencies is shown in Fig. 7. Plot between $1/T$ and ln(σ_{ac}) gives the value of activation energy. According to Arrhenius principle

$$\sigma_{ac} = \sigma_o \exp\left(\frac{-E_a}{K_B T}\right) \tag{6}$$

where σ_o = pre-exponential factor, E_a = activation energy, K_B is Boltzmann constant and T is the absolute temperature.

Values of activation energy for different Gd content at 10 kHz and at low (280–333 K) and high (400–500 K)

Table 2
Variation of activation energy obtained from AC process at low (300 K) and high (450 K) temperature ranges for 10 kHz.

Sample name	Activation energy (eV) at 10 kHz	
	300 K	450 K
S0	0.73	0.023
S2	1.02	0.414
S4	0.99	0.623
S6	0.98	0.767
S8	0.89	0.738
S10	0.71	0.585

temperature regimes are given in Table 2. At high temperature side, activation energy is greatly reduced because thermal energy has greater role in affecting charge carriers' movement.

In $CaCu_3Ti_4O_{12}$ ceramics, Ti^{3+} and Ti^{4+} can form Ti^{3+}–O–Ti^{4+} bond. Ti-3d electron can hop from Ti^{3+} to Ti^{4+} under applied field. Being larger in size Ti^{3+} ion will distort the lattice and will produce polaronic distortion [21].

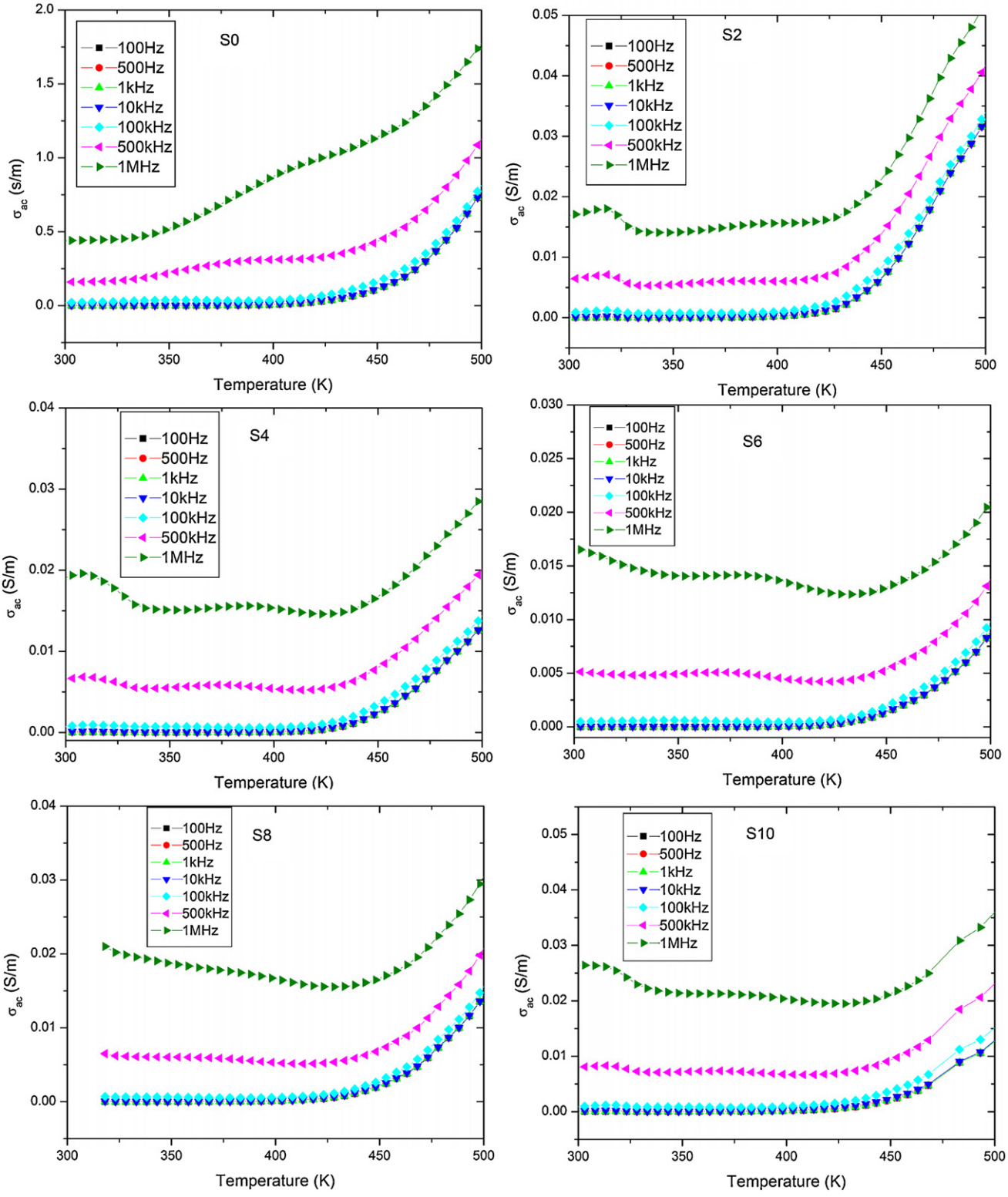

Fig. 6. Variation of AC conductivity σ_{ac} with temperature at different for pure and Gd doped CCTO samples.

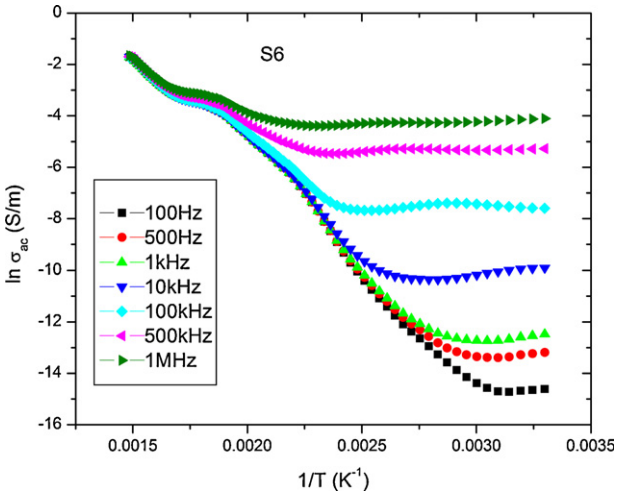

Fig. 7. Arrhenius plot between $1/T$ and ln σ_{ac} for Gd doped sample S6.

4. Conclusion

It is observed that grain size is greatly affected and decreases by substitution of Gd in CCTO. Dielectric constant decreases with Gd substitution. Decrease in dielectric constant in MHz region may be attributed to high frequency dielectric relaxation due to Maxwell–Wagner effect arising from the charge accumulation at interface of materials with different conductivities. Doped samples show smaller value of dielectric loss in the middle frequency range (∼10 kHz–1 MHz) and in the temperature range 300–400 K. Dispersion in dielectric loss at lower frequencies may be arising from electrode polarization. At lower frequencies, σ_{ac} is close to DC conductivity and conduction is of long range behaviour while at high frequency, long range motion cannot occur. With increase in temperature, activation energy is greatly reduced due to thermal energy gained by charge carriers at elevated temperature therefore an increase in conductivity is observed at higher temperature.

References

[1] C.C. Homes, T. Vogt, S.M. Shapiro, S. Wakimoto, A.P. Ramirez, Optical response of high-dielectric-constant perovskite-related oxide science, Science 293 (2001) 673–676.

[2] M.A. Subramanian, D. Li, N. Duan, B.A. Reisner, A.W. Sleight, High dielectric constant in $ACu_3Ti_4O_{12}$ and $ACu_3Ti_3FeO_{12}$ phases, J. Solid State Chem. 151 (2000) 323–325.

[3] D.C. Sinclair, T.B. Adams, F.D. Morrison, A.R. West, $CaCu_3Ti_4O_{12}$: one-step internal barrier layer capacitor, Appl. Phys. Lett. 80 (2002) 2153–2155.

[4] T.B. Adams, D.C. Sinclair, A.R. West, Giant barrier layer capacitance effects in $CaCu_3Ti_4O_{12}$ ceramics, Adv. Mater. 14 (2002) 1321–1323.

[5] P. Lunkenheimer, R. Fichtl, S.G. Ebbinghaus, A. Loidl, Nonintrinsic origin of the colossal dielectric constants in $CaCu_3Ti_4O_{12}$, Phys. Rev. B 70 (2004), 172102(1–4).

[6] T.B. Adams, D.C. Sinclair, A.R. West, Influence of processing conditions on the electrical properties of $CaCu_3Ti_4O_{12}$ ceramics, J. Am. Ceram. Soc. 89 (2006) 3129–3135.

[7] R. Kashyap, O.P. Thakur, N.C. Mehra, R.P. Tandon, Effect of processing conditions on dielectric properties of $CaCu_3Ti_4O_{12}$ ceramics, Int. J. Mod. Phys. B 25 (8) (2011) 1049–1059.

[8] J. Li, M.A. Subramanian, H.D. Rosenfeld, C.Y. Jones, B.H. Toby, A.W. Sleight, Clues to the giant dielectric constant of $CaCu_3Ti_4O_{12}$ in the defect structure of $SrCu_3Ti_4O_{12}$, Chem. Mater. 16 (2004) 5223–5225.

[9] B. Shri Prakash, K.B.R. Varma, Ferroelectric like and pyroelectric behavior of $CaCu_3Ti_4O_{12}$ ceramics, Appl. Phys. Lett. 90 (2007), 082903(1–3).

[10] R. Kashyap, T. Dhawan, P. Gautam, O.P. Thakur, N.C. Mehra, R.P. Tandon, Effect of processing conditions on electrical properties of $CaCu_3Ti_4O_{12}$ ceramics, Mod. Phys. Lett. B 24 (12) (2010) 1267–1273.

[11] L.E. Cross, Relaxor ferroelectrics, Ferroelectrics 76 (1987) 241.

[12] B.S. Prakash, K.B.R. Varma, Effect of sintering conditions on the dielectric properties of $CaCu_3Ti_4O_{12}$ and $La_{2/3}Cu_3Ti_4O_{12}$ ceramics: a comparative study, Physica B 382 (2006) 312–319.

[13] G. Blatter, F. Greuter, Carrier transport through grain boundaries in semiconductors, Phys. Rev. B 33 (1986) 3952–3966.

[14] T.B. Adams, D.C. Sinclair, A.R. West, Characterization of grain boundary impedances in fine- and coarse-grained $CaCu_3Ti_4O_{12}$ ceramics, Phys. Rev. B 73 (2006), 094124(1–9).

[15] L.F. Xu, P.B. Qi, X.P. Song, X.J. Luo, C.P. Yang, Dielectric relaxation behaviors of pure and Pr_6O_{11}-doped $Cu_3Ti_4O_{12}$ ceramics in high temperature range, J. Alloys Compd. 509 (2011) 7697–7701.

[16] X.-J. Luo, C.P. Yang, S.S. Chen, X.P. Song, H. Wang, K. Baerner, The trap state relaxation related polarization in $Cu_3Ti_4O_{12}$, J. Appl. Phys. 108 (2010), 014107(1–5).

[17] A.M.M. Farea, S. Kumar, K.M. Batoo, A. Yousef, Alimuddin, Influence of frequency, temperature and composition on electrical properties of polycrystalline $Co_{0.5}Cd_xFe_{2.5-x}O_4$ ferrites, Physica B 403 (2008) 684–701.

[18] S.R. Elliott, A.c. conduction in amorphous chalcogenide and pnictide semiconductors, Adv. Phys. 36 (1987) 135–217.

[19] C. León, A. Rivera, A. Várez, J. Sanz, J. Santamaria, K.L. Nagi, Origin of constant loss in ionic conductors, Phys. Rev. Lett. 86 (2001) 1279–1282.

[20] W. Li, R.W. Schwartz, Ac conductivity relaxation processes in $CaCu_3Ti_4O_{12}$ ceramics: grain boundary and domain boundary effects, Appl. Phys. Lett. 89 (2006), 242906(1–3).

[21] L. Zhang, Z.-J. Tang, Polaron relaxation and variable-range-hopping conductivity in the giant-dielectric-constant material $CaCu_3Ti_4O_{12}$, Phys. Rev. B 70 (2004), 174306(1–6).